Histol Histopathol (2023) 38: 1487-1498

Histology and Histopathology
From Cell Biology to Tissue Engineering

ORIGINAL ARTICLE Open Access

Long noncoding RNA FTX promotes epithelial-mesenchymal transition of epithelial ovarian cancer through modulating miR-7515/TPD52 and activating Met/Akt/mTOR

Yong Li[1,2*], Xinghua Zhu[3*], Can Zhang[1], Yi Yin[4], Lei Chen[2], Yushan Liu[3], Aiqin He[1] and Fei Xia[5]

[1]Department of Gynecological Oncology, Nantong Tumor Hospital, Affiliated Tumor Hospital of Nantong University, Nantong, [2]Department of Gynecology and Obstetrics, The First Affiliated Hospital of Soochow University, Suzhou, [3]Department of Pathology, Nantong Tumor Hospital, Affiliated Tumor Hospital of Nantong University, [4]Department of Gynecology and Obstetrics, Medical College of Nantong University, Nantong, [5]Reproductive Medicine Center, Department of Gynecology and Obstetrics, The First Affiliated Hospital of Soochow University, Suzhou, Jiangsu, China

*These authors contributed equally to this work

Summary. Overexpressed long noncoding RNA FTX is associated with low survival rate of epithelial ovarian cancer (EOC) patients, and enhances tumor infiltration. Thus, we aim to illuminate the undefined underlying mechanisms. Real-time quantitative polymerase chain reaction was applied to detect the expressions of FTX, miR-7515, miR-342-3p, miR-940, miR-150-5p, miR-205-5p and tumor protein D52 (TPD52). Cell counting kit-8 and transwell assays were utilized to explore the cell viability, migration or invasion of EOC cells. Western blot was conducted to measure the expressions of E-cadherin, N-cadherin, Met, phosphorylated (p)-Met, Akt, p-Akt, mTOR and p-mTOR. LncBase and TargetScan predicted the binding of miR-7515 with FTX, and the binding of TPD52 with miR-7515, respectively. The two bindings were further validated by dual luciferase reporter assay. As a result, FTX sponged miR-7515 and miR-7515 targeted to TPD52. FTX was overexpressed in four EOC cell lines. Overexpressed FTX enhanced the cell viability, migration or invasion of EOC cells, elevated N-cadherin and TPD52 expressions, phosphorylated Met/Akt/mTOR, and inhibited E-cadherin expression. All these influences were subsequently reversed by miR-7515 mimic. Collectively, FTX regulates miR-7515/TPD52 to facilitate the migration, invasion or epithelial-mesenchymal transition of EOC through activating Met/Akt/mTOR signaling pathway.

Key words: Epithelial ovarian cancer, FTX, miR-7515, TPD52, Epithelial-mesenchymal transition

Corresponding Author: Fei Xia, Reproductive Medicine Center, Department of Gynecology and Obstetrics, The First Affiliated Hospital of Soochow University, 899 Pinghai Road, Suzhou, Jiangsu Province, 215006, PR China. e-mail: xiafei_fxia@163.com and Aiqin He, Department of Gynecological Oncology, Nantong Tumor Hospital, Affiliated Tumor Hospital of Nantong University, 30 Tongyang North Road, Pingchao Town, Tongzhou District, Nantong, Jiangsu Province, 226361, China. E-mail: haq0118@163.com

www.hh.um.es. DOI: 10.14670/HH-18-620

Introduction

Ovarian cancer (OC) is the seventh most commonly diagnosed cancer type and most deadly gynecologic cancer globally, and only approximately 46% OC patients survive after diagnosis (Siegel et al., 2016; Doherty et al., 2017). Epithelial ovarian cancer (EOC) refers to advanced ovarian cancer, and is a cohort of tumor types dominated by high grade serous ovarian cancer (HGSOC) (Konecny et al., 2014). EOC can be classified into type I and type II subtypes according to distinguishing prognosis, and type II EOC with greater invasiveness can be further divided into HGSC, high-grade endometrioid or a few undifferentiated carcinomas (Lengyel, 2010; Kurman and Shih Ie, 2011; Ali et al., 2013; Kurman, 2013). Current early diagnosis for EOC depends on molecular strategies, and there is an urgent need to develop effective methods based on biomarkers (Yang et al., 2017; Lheureux et al., 2019). Hence, we need to probe into the underlying functions of some research targets towards EOC, and unveil the underlying action mechanism.

Through bioinformatic analysis for the competing

endogenous RNA networks in HGSOC, overexpressed lncRNA FTX was found to be correlated with shortened overall survival rate of patients and increased lymphocyte infiltration level (Wu et al., 2020). No previous studies have focused on the association between FTX and OC. Notably, FTX has been frequently suggested to act as a tumor promoter in many other cancers including gastric cancer, colorectal cancer, lung adenocarcinoma and osteosarcoma (Li et al., 2018a, 2019; Zhang et al., 2018, 2020; Huang et al., 2020; Huo et al., 2020; Zhao et al., 2020). Therefore, it is worth revealing the detailed effects of FTX on EOC.

Moreover, the modulation of related signaling pathways is worthy of investigation. LncRNA FTX has been confirmed to block the metastasis or epithelial-mesenchymal transition (EMT) of endometrial stromal cells through inhibiting the phosphorylation of PI3K or Akt (Wang et al., 2020a). In thyroid cancer, lncRNA XIST, the effector of FTX, provoked cell proliferation or tumor growth by activating Met/PI3K/Akt signaling pathway (Liu et al., 2018). In view of this, it is plausible that FTX could directly or indirectly modulate the activation of PI3K and Akt and potential Met.

According to former findings, genetic and stromal cells in tumors are spatio-temporal heterogeneous under tumor microenvironment (Joyce and Pollard, 2009; McGranahan and Swanton, 2017). Malignant epithelial cells are prone to EMT to acquire heterogenous traits of mesenchymal cells, and then disseminate from primary tumors and metastasize to distant sites, especially through capillary sized vessels (Thiery and Sleeman, 2006; Ye and Weinberg, 2015; Au et al., 2016). This process is primarily modulated by TGF-β signaling which is over-activated by cancer-associated fibroblasts (Calon et al., 2014; Zhuang et al., 2015), and is also regulated by c-Met tumor promoter (Chang et al., 2019). In a previous study, overexpressed Met was down-regulated by microRNA (miRNA, miR)-338-3p, accompanied by the attenuated tumor proliferation or aggressiveness and the inactivated downstream Wnt/catenin or MEK/ERK signaling pathway (Zhang et al., 2019), implying that miRNAs have potential in modulating Met to affect downstream EMT progression. Given the above information, we aimed to explore potential miRNAs regulated by lncRNA and construct the modulatory network, and reveal the associated morphological alterations such as EOC migration or invasion.

Materials and methods

Cell culture

Human ovarian epithelial cell line HOSE (7310) was purchased from Shanghai Zhong Qiao Xin Zhou Biotechnology Co., Ltd (https://www.zqxzbio.com/Index/p_more/pid/166.html). Human OC cell lines CAOV3 (HTB-75), SKOV3 (HTB-77), OVCAR3 (HTB-161) and ES-2 (CRL-1978) were obtained from American Type Culture Collection (ATCC, Manassas, VA, USA). All cells were cultivated in a 5% CO_2 incubator (3110, Thermo Fisher Scientific, Waltham, MA, USA) at 37°C. CAOV3 cells were grown in Dulbecco's Modified Eagle's Medium (DMEM, 30-2002, ATCC) supplemented with 10% fetal bovine serum (FBS, 10099, Gibco, Waltham, MA, USA) and 100 U/mL of penicillin and 100 μg/mL streptomycin (1% P/S, 15140122, Gibco). SKOV3 and ES-2 cells were maintained in modified McCoy's 5a Medium (30-2007, ATCC) containing 10% FBS and 1% P/S. HOSE and OVCAR3 cells were cultured in RPMI1640 medium (30-2001, ATCC) blended with 10%-20% FBS and 1% P/S as needed. Cells in 3-10 passages were used in our research.

Cell transfection

MiR-7515 mimic (M, AGAAGGGAAGAUGGUGAC), mimic negative control (MC, UUCUUCGAACGUGUCACGUTT), miR-7515 inhibitor (I, GUCACCAUCUUCCCUUCU), and inhibitor negative control (IC, CAGUACUUUUGUGUAGUACAA) were acquired from Thermo Fisher Scientific (Carlsbad, CA, USA). Overexpression plasmids for FTX were constructed by inserting whole sequence of FTX into the pcDNA 3.1 vector (V79020, Invitrogen, Carlsbad, CA, USA). Empty vector was used as negative control (NC). Short hairpin RNA (shRNA) targeting FTX (shFTX, target sequence: CTACTGCTGAAGAGGTATATT) (C02001) was acquired from GenePharma Corporation (Shanghai, China), and empty vector was used as negative control (shNC). Based on the provider's instructions, EOC cells were cultured overnight in advance. Next day, the original medium was replaced by fresh DMEM or modified McCoy's 5a medium without FBS and the above-mentioned plasmids with Lipofectamine 2000 reagent compound (11668027, Invitrogen). Complete medium containing half FBS contents was used the following day.

Cell counting kit-8 (CCK-8) assay

CCK-8 assay (CK04, Donjindo, Tokyo, Japan) was conducted to evaluate viability of EOC cells under the transfection of shFTX, FTX overexpression plasmid or their negative controls. Cells without transfection were set as control group. Cells were seeded in 96-well plates (5000 cells/well), and the experiments were repeated in triplicate. After diverse treatment for 24-72 hours (h), 10 μL CCK-8 solution was added into each well, followed by culture in CO_2 incubator at 37°C for another 4h. Finally, the OD^2 value was read at 450 nm by a microplate reader (Sunrise, Tecan, Austria) to measure cell viability.

Bioinformatic analysis and dual luciferase reporter assay

Various targets, which were predicted to bind FTX through LncBase (http://carolina.imis.athena-innovation.gr/diana_tools/web/index.php?r=lncbasev2/index-

predicted), were screened using miTG score, and five targets were selected. The expressions of miR-7515, miR-342-3p and miR-940 in five targets were found to be significantly altered by modulating FTX expression. Of them, the change of miR-7515 expression was the most obvious. LncBase was further applied to predict the binding of miR-7515 with FTX. TargetSacn (http://www.targetscan.org/vert_72/) was used to predict the binding of tumor protein D52 (TPD52) with miR-7515.

Mutant type FTX sequence with altered binding sites for miR-7515, wild type FTX sequence, mutant type TPD52 sequence with altered binding sites for miR-7515 and wild type TPD52 sequence were all synthesized by GenePharma (Shanghai, China). The sequences were inserted into pmirGLO dual luciferase miRNA target expression vector (E1330, Promega, madison, WI, USA). In researching the binding of FTX or TPD52 with miR-7515, SKOV3 or CAOV3 cells in mimic group were co-transfected with pmirGLO-FTX/TPD52-WT or pmirGLO-FTX/TPD52-MUT reporter plasmid along with miR-7515 mimic. SKOV3 or CAOV3 cells in mimic control group were co-transfected with pmirGLO-FTX/TPD52-WT or pmirGLO-FTX/TPD52-MUT reporter plasmid along with mimic control. The transfection was carried out with Lipofectamine 2000 reagent (11668027, Invitrogen). Firefly and Renilla luciferase activities were detected based on GloMax 96 Microplate Luminometer with Dual Injectors (E6521, Promega). The Renilla luciferase activity was considered as the internal reference.

Transwell assay

A conventional 24-well Transwell system (3464, 8.0 μm pore, Corning) was used to measure the migration ability of EOC cells. Detection of invasive ability was further conducted using Transwell system covered with a Max Gel ECM (E0282, Sigma-Aldrich). Each well of the Transwell system includes an upper chamber and a lower chamber. 100 μL SKOV3 or CAOV3 cell suspension containing 1×10^5 cells without FBS was inoculated into the upper chamber. Then each lower chamber was filled with 600 μL complete medium supplemented with 20% FBS. After 48h of incubation, cells passing through the membrane were fixed with 4% paraformaldehyde (P0099, Beyotime, Shanghai, China) at 25°C for 30 min and then dyed with 0.1% crystal violet solution (G1063, Solarbio) for 20 min. The excessive staining was washed by PBS (02-024-1A, Biological industry, Connecticut, USA). Cells remaining at the upper side of filters were gently removed with cotton swabs. The dyeing pictures were taken by the microscope (CKX41, Olympus, Shinjuku, Tokyo, Japan) at × 250 magnification.

Real-time quantitative polymerase chain reaction (RT-qPCR) assay

Total RNA was isolated from EOC cells using TRIzol Reagent (15596026, Invitrogen) and reversely transcribed into cDNA by reverse transcription reagents (AH401-01, TransGen, Beijing, China; MR101-01, Vazyme, Nanjing, China). Next, SYBR Green Real-Time PCR Master Mix (AQ301-01, TransGen) and primers were used to detect the gene expression using CFX Opus Real-time PCR system (CFX96, Bio-rad, CA, USA). The results were calculated according to $2^{-\Delta\Delta Ct}$ method (Livak and Schmittgen, 2001), with GAPDH or U6 as the internal reference.

The primers of FTX were Forward (F): 5'-TCC TGTGCCTGCTGTCCATT-3', Reverse (R): 5'-CTTAG AGCTGGCCGTCCCAA-3'. The primers of TPD52 were F: 5'-ATTGCCAAAGGGTGGCAAGA-3', R: 5'-AAAAGCAGCTGAGGCCTTCT-3'. The relative expressions of these genes were calculated based on the GAPDH expression using the following primers, F: 5'-ACATGGCTGAGAACGGGAAG-3', R: 5'-TCGCCCC ACTTGATTTTGGA-3'. The primers of miR-7515 were F: 5'-TGACGTCGTATCCAGTGCAA-3', R: 5'-GTCGTATCCAGTGCGTGTCG-3'. The primers of miR-342-3p were F: 5'-AAATCGCACCCGTGTCG TAT-3', R: 5'-GTATCCAGTGCGTGTCGTGG-3'. The primers of miR-940 were F: 5'-CCCGTCGTATCCA GTGCAAT-3', R: 5'-GTCGTATCCAGTGCGTGTCG-3'. The primers of miR-150-5p were F: 5'-CCCAACC CTTGTACCAGTGG-3', R: 5'-TGTCGTGGAGTCG GCAATTG-3'. The primers of miR-205-5p were F: 5'-CATTCCACCGGAGTCTGGTC-3', R: 5'-TGTCGTG GAGTCGGCAATTG-3'. The relative expressions were calculated based on the U6 expression using the following primers, F: 5'-GCTTCGGCAGCACATAT ACTAAAAT-3', R: 5'-CGCTTCACGAATTTGCG TGTCAT-3'.

Western blot assay

Total protein in EOC cells was extracted using the radio immunoprecipitation assay (RIPA) lysis buffer (P0013B, Beyotime) supplemented with protease and phosphatase inhibitor (P1051, Beyotime) and 0.1 mM phenylmethylsulfonyl fluoride (PMSF, ST506, Beyotime). BCA protein assay kit (P0010, Beyotime) was utilized to determine total protein concentration. All protein samples to be used were diluted to a certain concentration. Then equal volumes of proteins were separated by sodium dodecyl sulfate-polyacrylamide gel electrophoresis (SDS-PAGE) (P0012A, Beyotime). After that, proteins were transferred onto polyvinylidene fluoride (PVDF) membrane (IPSN07852, Millipore, Bedford, MA, USA). The membrane was blocked with 5% nonfat milk at 4°C overnight, and then cut into strips.

Membrane strips were incubated with primary antibodies including those against E-cadherin (ab40772, 97 kDa, dilution 1:10000, Abcam, Cambridge, MA, USA), N-cadherin (ab18203, 130 kDa, dilution 1:1000, Abcam), Met (ab51067, 160 kDa, dilution 1:1000, Abcam), p-Met (ab68141, 156 kDa, dilution 1:1000,

Abcam), Akt (ab8805, 55 kDa, dilution 1:500, Abcam), p-Akt (ab38449, 56 kDa, dilution 1:1000, Abcam), mTOR (ab2732, 289 kDa, dilution 1:2000, Abcam), p-mTOR (ab109268, 289 kDa, dilution 1:1000, Abcam) and GAPDH (ab8245, 36 kDa, dilution 1:1000, Abcam), at 4°C overnight. Next, the membrane strips were washed by 0.1 M TBS containing 0.1% Tween-20 (TBST, ST673, Beyotime) three times, and further incubated with Horseradish Peroxidase (HRP)-conjugated secondary antibodies (ab205718, ab205719, dilution 1:5000 Abcam) at room temperature for 2h. Specific protein signals were examined using UltraSignal ECL Western Blotting Substrate (4AW011-200, 4A Biotech, Beijing, China), and quantified using Image J software (Wayne Rasband, NIH, USA).

Statistical analysis

All groups of data were analyzed by Graphpad Prism 8.0 (GraphPad Software Inc, La Jolla, CA, USA). The data were described by mean ± standard deviation (SD). The difference between EOC tumor group and normal group was analyzed by independent-samples *t*-test, and that among multiple groups was analyzed using one-way analysis of variance (ANOVA). Tukey's multiple comparison test was conducted as post hoc test. Chi-square test and rank sum test were used for counting data. Overall survival rate was estimated using the

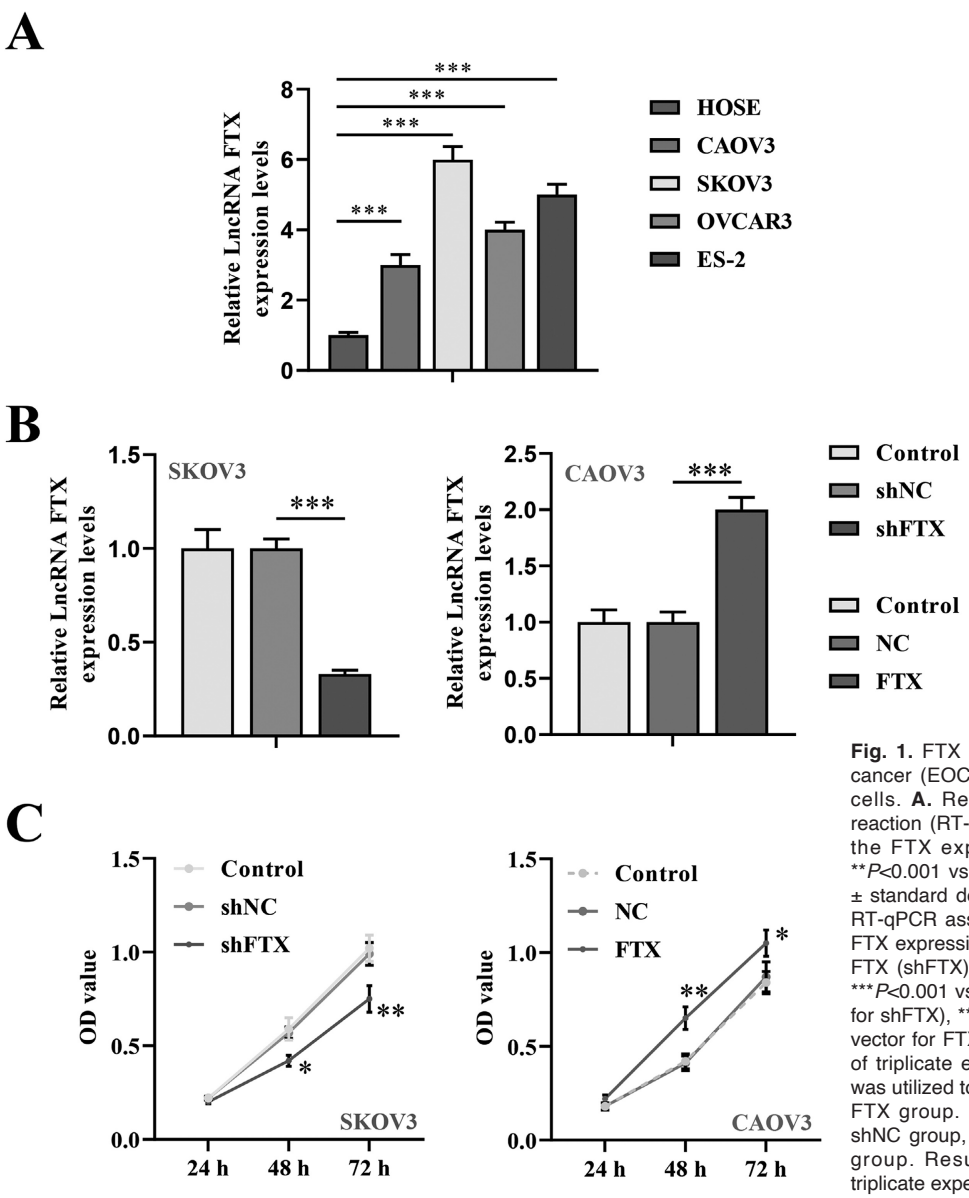

Fig. 1. FTX was overexpressed in epithelial ovarian cancer (EOC) cell lines and affected viability of EOC cells. **A.** Real-time quantitative polymerase chain reaction (RT-qPCR) assay was conducted to measure the FTX expression level in four EOC cell lines. ***P*<0.001 vs. HOSE. Results are described as means ± standard deviation (SD) of triplicate experiments. **B.** RT-qPCR assay was applied to detect the changes of FTX expression caused by short hairpin RNA targeting FTX (shFTX) and FTX overexpression plasmid (FTX). ****P*<0.001 vs. sh negative control (shNC, empty vector for shFTX), ****P*<0.001 vs. negative control (NC, empty vector for FTX). Results are described as means ± SD of triplicate experiments. **C.** Cell counting kit-8 assay was utilized to determine cell viability in shFTX group or FTX group. **P*<0.05 vs. shNC group, ***P*<0.01 vs. shNC group, **P*<0.05 vs. NC group, ***P*<0.01 vs. NC group. Results are described as means ± SD of triplicate experiments.

Kaplan-Meier method, and the difference between two parallel groups was analyzed through Log-Rank test. $P<0.05$ was considered as statistical significance.

Results

FTX was overexpressed in EOC cell lines, and FTX knockdown inhibited the viability of EOC cells

FTX expression level was higher in four EOC cell lines than in normal ovarian epithelial cells (Fig. 1A, $P<0.001$). Transfection of shFTX down-regulated FTX expression in SKOV3 cells, and transfection of FTX overexpression plasmid up-regulated the FTX expression in CAOV3 cells (Fig. 1B, $P<0.001$). According to CCK-8 assay results, the viability of EOC cells was inhibited by FTX knockdown while being significantly promoted by FTX overexpression (Fig. 1C, $P<0.05$).

FTX knockdown suppressed the migration, invasion and EMT process of EOC cells

Similarly, the results of transwell assay revealed that FTX knockdown impeded migration and invasion of EOC cells, while FTX overexpression generated the opposite effects (Fig. 2A,B, $P<0.001$). Besides, FTX knockdown remarkably increased E-cadherin expression and decreased N-cadherin expression, while FTX overexpression decreased E-cadherin expression and increased N-cadherin expression (Fig. 3A,B, $P<0.001$).

MiR-7515 was predicted and validated to bind to FTX

Various targets of FTX, which were predicted through LncBase, were screened out according to miTG score, and five targets were selected. Among them, the expressions of miR-7515, miR-342-3p and miR-940 were found to be evidently affected with the changes of FTX expression, and the expression change of miR-7515 was the most remarkable (Fig. 3C,D, $P<0.05$). MiR-7515 was further predicted to bind to FTX through LncBase (Fig. 4A), and dual luciferase assay results further validated the binding of miR-7515 with FTX (Fig. 4B, $P<0.001$).

MiR-7515 inhibitor reversed the effects of FTX knockdown and miR-7515 mimic offset the effects of FTX overexpression on migration or invasion of EOC cells

FTX knockdown resulted in up-regulation of miR-7515, while miR-7515 inhibitor decreased miR-7515 expression and reversed the effect of FTX knockdown

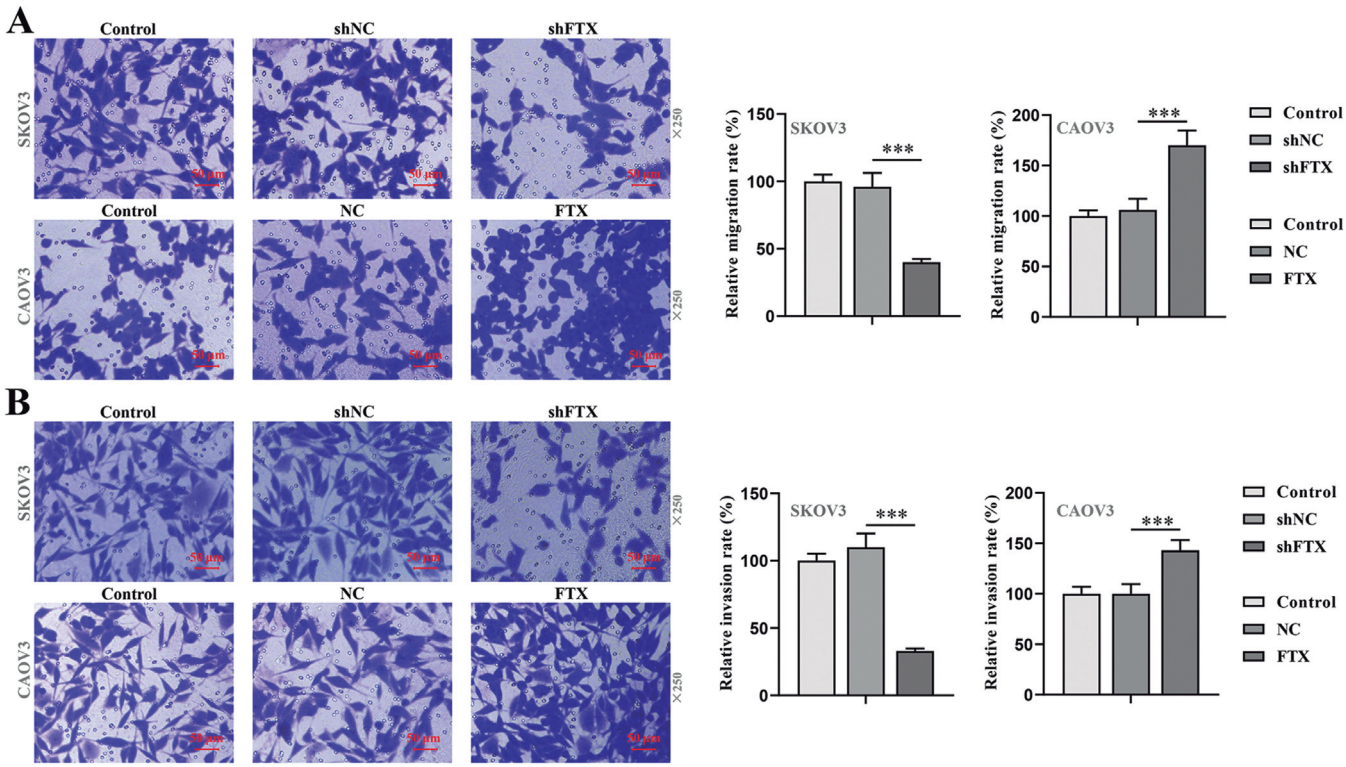

Fig. 2. Altered FTX expression changed the cell migration or invasion of EOC cells. **A, B.** Transwell assay was applied to detect the migration or invasion in shFTX group or FTX group. ***$P<0.001$ vs. shNC group, ***$P<0.001$ vs. NC group. Results are described as means ± SD of triplicate experiments.

(Fig. 5A, $P<0.001$). Moreover, FTX overexpression brought about down-regulation of miR-7515, while miR-7515 mimic elevated miR-7515 expression and offset the effect of FTX overexpression (Fig. 5B, $P<0.001$). In line with transwell assay results, FTX knockdown hindered migration and invasion of EOC cells, but miR-7515 inhibitor facilitated those of EOC cells and reversed the function of FTX knockdown (Fig, 5C,c, $P<0.01$). Also, FTX overexpression enhanced migration and invasion of EOC cells, whilst miR-7515 mimic blocked those of EOC cells and neutralized the function of FTX overexpression (Fig. 5D,d, $P<0.05$).

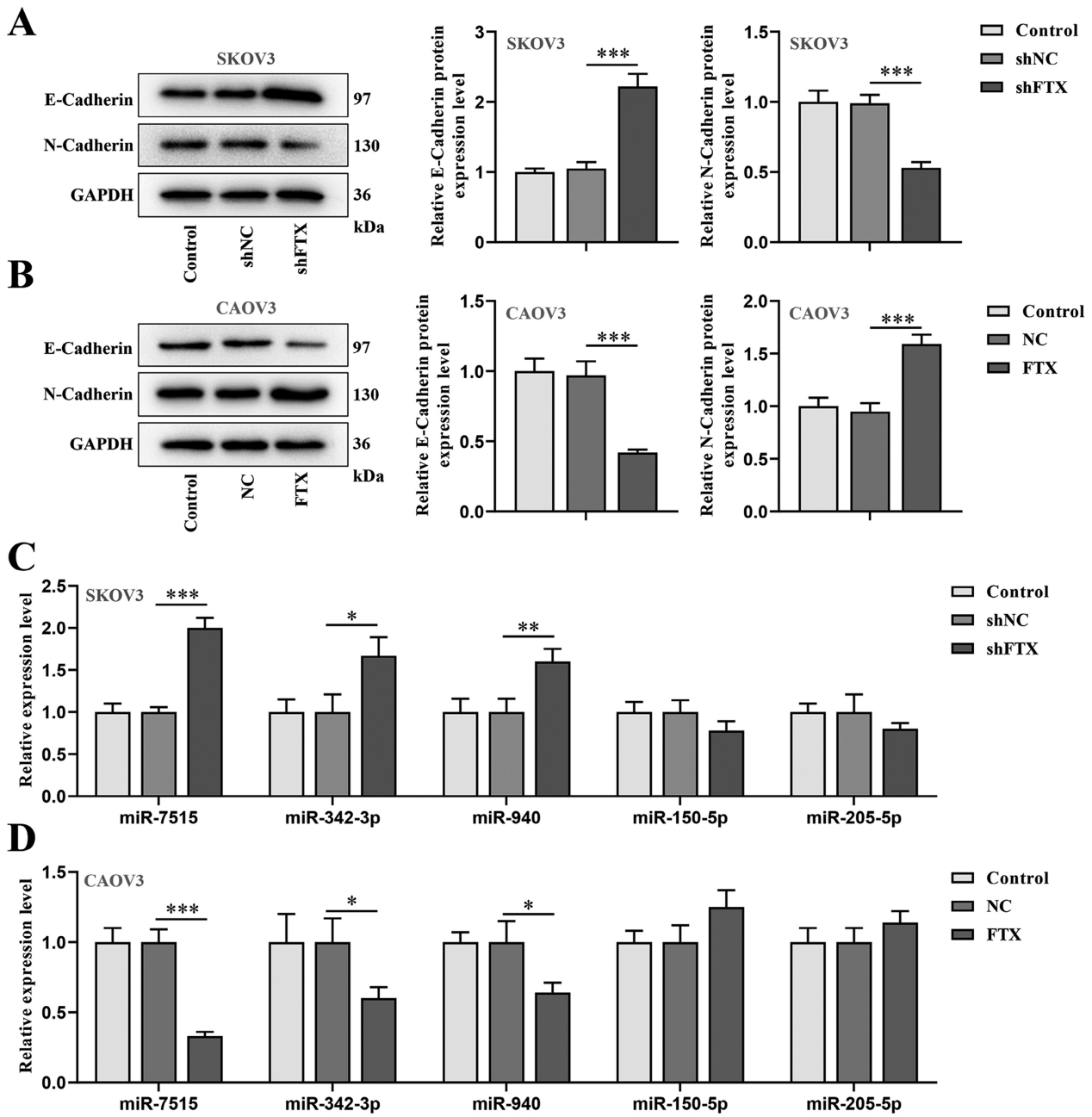

Fig. 3. E-cadherin and N-cadherin expressions were altered as FTX expression changed and expressions of serial predicted microRNAs (miRNAs) were detected. **A, B.** Western blot (WB) assay was employed to detect E-cadherin or N-cadherin expression in shFTX group or FTX group. ***$P<0.001$ vs. shNC group, ***$P<0.001$ vs. NC group. Results are described as means ± SD of triplicate experiments. **C, D.** RT-qPCR assay was performed to quantify the expressions of miR-7515, miR-342-3p, miR-940, miR-150-5p and miR-205-5p. *$P<0.05$ vs. shNC group, **$P<0.01$ vs. shNC group, ***$P<0.001$ vs. shNC group, *$P<0.05$ vs. NC group, ***$P<0.001$ vs. NC group. Results are described as means ± SD of triplicate experiments.

MiR-7515 inhibitor counteracted the effects of FTX knockdown and miR-7515 mimic reversed the effects of FTX overexpression on expressions of EMT markers and activation of Met, Akt or mTOR

FTX knockdown blocked the EMT process of EOC cells through elevating E-cadherin expression and reducing N-cadherin expression; however, miR-7515 inhibitor promoted the EMT process and reversed the effect of FTX knockdown (Fig. 6A, $P<0.05$). FTX overexpression facilitated the EMT process of EOC cells via reducing E-cadherin expression and augmenting N-cadherin expression, but miR-7515 mimic blocked the EMT process and offset the effect of FTX overexpression (Fig. 6B, $P<0.05$). In addition, FTX knockdown starkly inhibited the phosphorylation of Met, Akt and mTOR, which was counteracted by miR-7515 inhibitor (Fig. 6C, $P<0.01$). FTX overexpression remarkably promoted the phosphorylation of Met, Akt and mTOR, which was neutralized by miR-7515 mimic (Fig. 6D, $P<0.01$).

TPD52 was predicted and validated to bind to miR-7515

TPD52 was predicted and validated to bind to miR-7515 (Fig. 7A,B, $P<0.001$). It can be noted that FTX knockdown decreased TPD52 expression, while miR-7515 inhibitor increased TPD52 expression and reversed the effect of FTX knockdown (Fig. 7C, $P<0.01$). FTX overexpression increased TPD52 expression, but miR-7515 mimic produced the opposite effect and neutralized the influence of FTX overexpression (Fig. 7C, $P<0.01$).

Discussion

In the current study, overexpressed FTX promoted migration, invasion and EMT process. MiR-7515 was detected to bind to FTX and the sponge of FTX towards miR-7515 enhanced the EMT and the phosphorylation of Met/Akt/mTOR signaling. TPD52 acted as the downstream effector.

The migration and invasion of EOC cells, which represent the aggressiveness of tumors, were related to FTX expression. The molecular mechanism may involve the promotion of EMT, which was achieved by overexpressed FTX to decline E-cadherin expression and elevate N-cadherin expression. EMT, a calcium-related pathogenic pathway in OC, can be blocked by intracellular calcium chelator, after which lung metastasis is alleviated and the survival period of SKOV3 xenograft mice is prolonged (Liu et al., 2019). Against the background of promising effects achieved by anti-EMT treatment in attenuating the drug resistance of OC (Loret et al., 2019), we determined to investigate the EMT-associated potential signaling pathway, so as to find strategies for inhibiting the tumorigenesis or metastasis of EOC.

The hormones or growth factors secreted by ovary, such as TGF-β or activin A, can stimulate the activation of non-canonical PI3K/Akt signaling pathway to provoke EMT process, and promote the progression of HGSOC (Dean et al., 2017). Hence, PI3K/Akt signaling pathway plays a pivotal role in the early stage of HGSOC (Dean et al., 2017). In this study, we discovered that FTX sponged miR-7515, and revealed that the

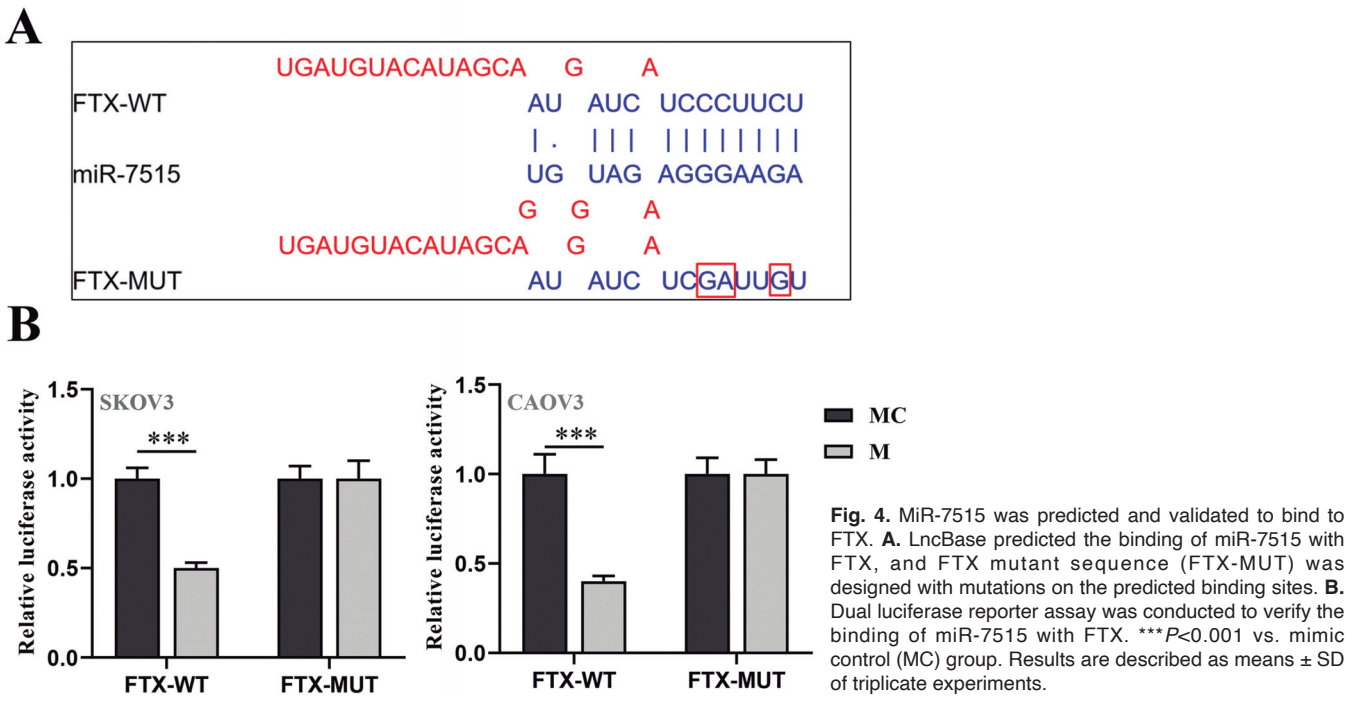

Fig. 4. MiR-7515 was predicted and validated to bind to FTX. **A.** LncBase predicted the binding of miR-7515 with FTX, and FTX mutant sequence (FTX-MUT) was designed with mutations on the predicted binding sites. **B.** Dual luciferase reporter assay was conducted to verify the binding of miR-7515 with FTX. ***$P<0.001$ vs. mimic control (MC) group. Results are described as means ± SD of triplicate experiments.

binding of FTX and miR-7515 mediated EMT progression and the activation of Met, Akt and mTOR. Previous research indicated that miR-206 mimic disrupts the phosphorylation of c-Met/Akt/mTOR pathway to attenuate cell growth and invasion, and promote cell cycle arrest and apoptosis in EOC (Dai et al., 2018). Meanwhile, PI3K/Akt/mTOR signaling can elevate expression levels of cancer stem cell biomarkers, accelerate the EMT of EOC and enhance the chemoresistance of EOC towards cisplatin treatment,

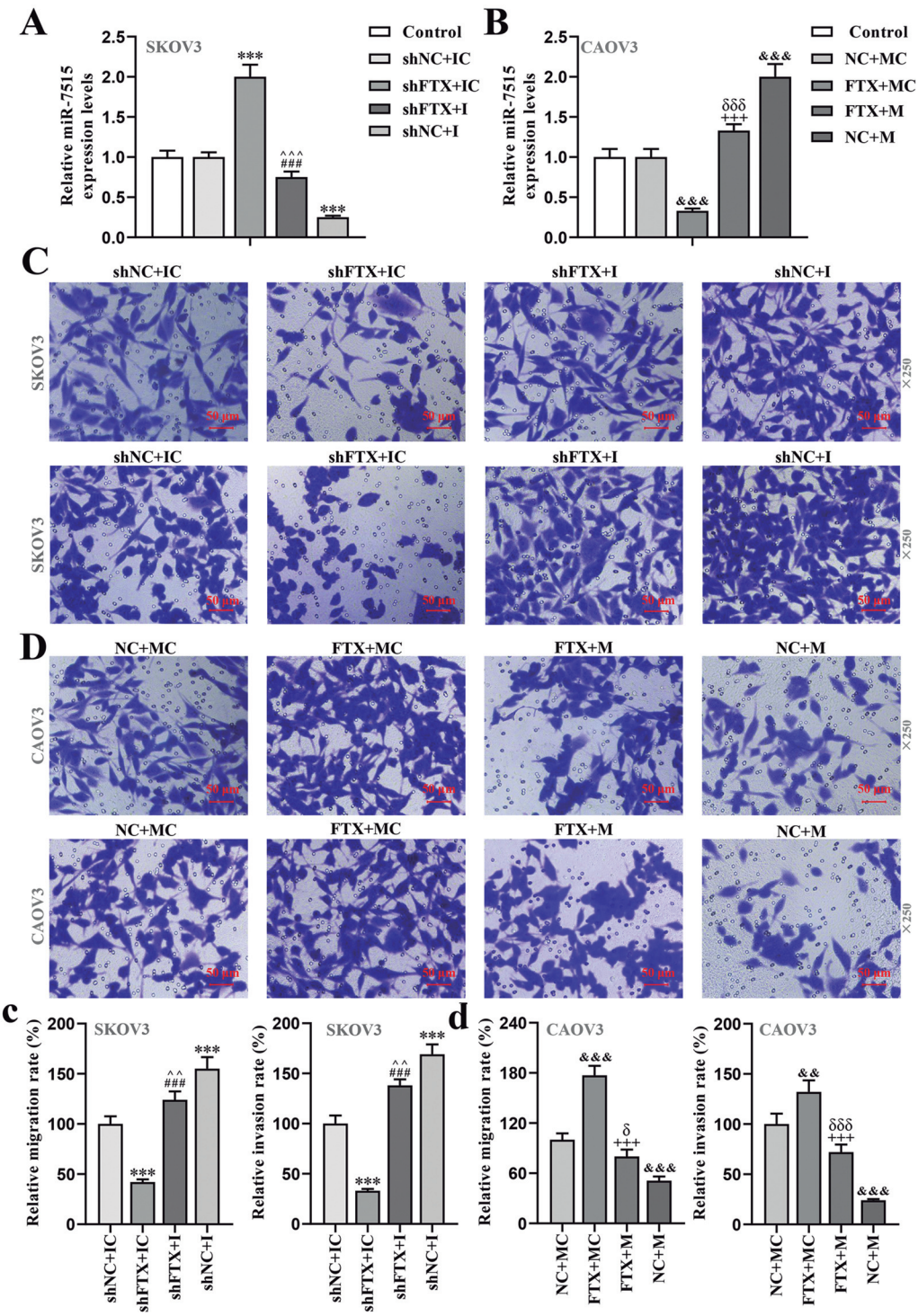

Fig. 5. MiR-7515 inhibitor reversed the effects of FTX knockdown and miR-7515 mimic reversed the effects of FTX overexpression on cell migration and invasion of EOC cells. **A.** RT-qPCR assay was applied to measure miR-7515 expression in cells transfected with shFTX or miR-7515 inhibitor (I) or their combination. ***P<0.001 vs. shNC+inhibitor control (IC) group, ###P<0.001 vs. shFTX+IC group, ^^^P<0.001 vs. shNC+I group. Results are described as means ± SD of triplicate experiments. **B.** RT-qPCR assay was performed to measure miR-7515 expression in cells transfected with FTX overexpression plasmid or miR-7515 mimic (M) or their combination. &&&P<0.001 vs. NC+MC group, +++P<0.001 vs. FTX+MC group, δδδP<0.001 vs. NC+M group. Results are described as means ± SD of triplicate experiments. **C.** Transwell assay was carried out to determine the migration or invasion of EOC cells transfected with shFTX or miR-7515 inhibitor or their combination. ***P<0.001 vs. shNC+IC group, ###P<0.001 vs. shFTX+IC group, ^^P<0.01 vs. shNC+I group. Results are described as means ± SD of triplicate experiments. **D.** Transwell assay was performed to determine the migration or invasion of EOC cells transfected with FTX overexpression plasmid or miR-7515 mimic or their combination. &&P<0.01 vs. NC+MC group, &&&P<0.001 vs. NC+MC group, +++P<0.001 vs. FTX+MC group, δP<0.05 vs. NC+M group, δδδP<0.001 vs. NC+M group. Results are described as means ± SD of triplicate experiments.

through decreasing reactive oxygen species level (Deng et al., 2019). In addition, silencing of γ-glutamyl cyclotransferase, which is highly expressed in HGSOC, blocked the PI3K/Akt/mTOR axis to suppress the EMT process as well as the tumor growth or metastasis in vivo (Li et al., 2018b). The above findings reflect that the activation of Met, Akt or mTOR promotes EMT progression and other tumorigenic progressions of EOC. The regulatory effects of FTX and miR-7515 actually revealed their value in the treatments of EOC.

In addition, we established a FTX/miR-7515/TPD52 regulatory axis during the onset and development of

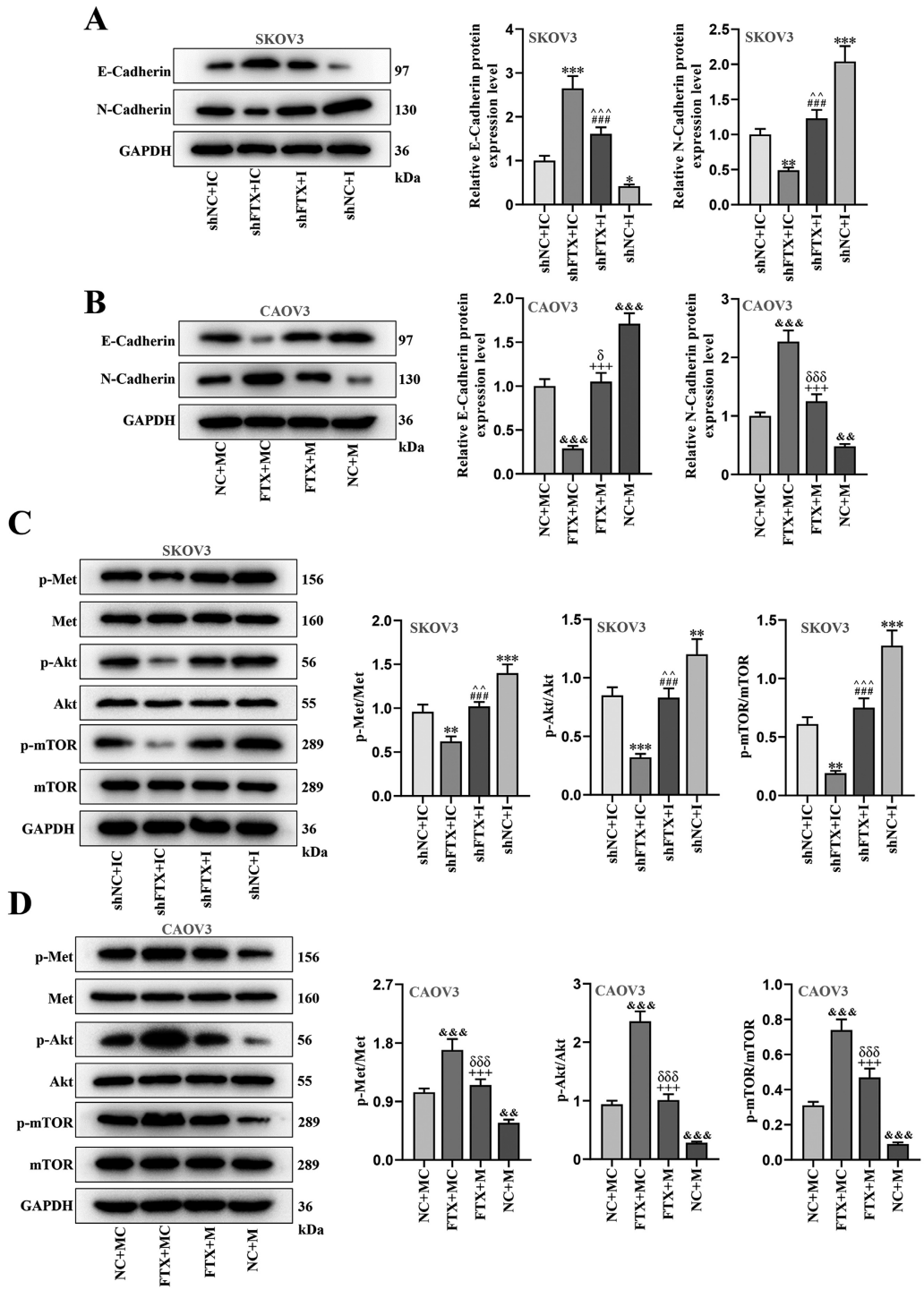

Fig. 6. MiR-7515 inhibitor reversed the effects of FTX knockdown and miR-7515 mimic offset the effects of FTX overexpression on EMT markers and activation of Met, Akt or mTOR. **A.** WB assay was performed to detect E-cadherin or N-cadherin expression in EOC cells transfected with shFTX or miR-7515 inhibitor or their combination. **P*<0.05 vs. shNC+IC group, ***P*<0.01 vs. shNC+IC group, ****P*<0.001 vs. shNC+IC group, ###*P*<0.001 vs. shFTX+IC group, ^^*P*<0.01 vs. shNC+I group, ^^^*P*<0.001 vs. shNC+I group. Results are described as means ± SD of triplicate experiments. **B.** WB assay was conducted to measure E-cadherin or N-cadherin expression in EOC cells transfected with FTX overexpression plasmid or miR-7515 mimic or their combination. &&*P*<0.01 vs. NC+MC group, &&&*P*<0.001 vs. NC+MC group, +++*P*<0.001 vs. FTX+MC group, δ*P*<0.05 vs. NC+M group, δδδ*P*<0.001 vs. NC+M group. Results are described as means ± SD of triplicate experiments. **C.** WB assay was performed to measure the expressions of Met, Akt and mTOR and their phosphorylation forms in EOC cells transfected with shFTX or miR-7515 inhibitor or their combination. ***P*<0.01 vs. shNC+IC group, ****P*<0.001 vs. shNC+IC group, ###*P*<0.001 vs. shFTX+IC group, ^^*P*<0.01 vs. shNC+I group, ^^^*P*<0.001 vs. shNC+I group. Results are described as means ± SD of triplicate experiments. **D.** WB assay was carried out to measure the expressions of Met, Akt and mTOR and their phosphorylation forms in EOC cells transfected with FTX overexpression plasmid or miR-7515 mimic or their combination. &&*P*<0.01 vs. NC+MC group, &&&*P*<0.001 vs. NC+MC group, +++*P*<0.001 vs. FTX+MC group, δδδ*P*<0.001 vs. NC+M group. Results are described as means ± SD of triplicate experiments.

EOC. Similar to our selection, miR-7515 was detected to be one of the four most remarkably down-regulated miRNAs in recurrent EOC compared with primary EOC, suggesting the close relation of miR-7515 with poor prognosis of EOC patients (Chong et al., 2015). This is the first article revealing the association between miR-7515 with OC, so our results are of great significance. In light of previous studies, miR-7515 plays different roles in lung cancer, pancreatic cancer and metastatic colorectal cancer (Lee et al., 2013; Francone et al., 2021; Huang et al., 2021; Lei et al., 2021). The suppressive functions of miR-7515 on the proliferation and migration of lung cancer cells are realized through targeting c-Met, which was similar to our results (Lee et al., 2013). TPD52 emerges as a tumor promoter in many kinds of tumors including cervical cancer, pancreatic cancer and triple negative breast cancer (Wang et al., 2019, 2020c; Lu et al., 2020; Shi et al., 2020a,b). TPD52 expression is higher in HGSOC than in serous borderline tumors, and TPD52 overexpression is related to the improved overall survival rate of patients with stage III serous OC, indicating that TPD52 expression is an independent prognostic index for OC (Byrne et al., 2010). In another article, TPD52 is recruited by LINC01133, and leads to the facilitated metastasis in EOC in vivo (Liu and Xi, 2020). Moreover, various competing endogenous RNA networks are found in the progression of OC, including PTAR/miR-101-3p/ZEB1, RHPN1-AS1/miR-596/LETM1 and OIP5-AS1/miR-137/ANF217, which focus on the EMT and metastasis of solid tumor types (Liang et al., 2018; Guo et al., 2020; Wang et al., 2020b). The oncogenic role of PTAR was especially validated to be linked to the pathogenic effects of TGF-β1 on the triggered EMT both in vitro and in vivo (Liang et al., 2018). The m6A modification maintains the stability of RHPN1-AS1 and enhances its sponging towards the tumor suppressor miR-596 to mediate the development of EOC (Wang et al., 2020b). Similar to the regulatory networks mentioned above, FTX, miR-7515 and TPD52 played unique roles in the disease, and their interactions greatly affected the development of EOC.

In conclusion, FTX sponged miR-7515 to promote TPD52 expression and facilitate the migration, invasion or EMT process of EOC cells through activating Met/Akt/mTOR signaling pathway. Our discovery fills the blank in which the modulatory role of FTX in EOC has not been previously reported. As the functions of FTX/miR-7515/TPD52 in the motility of EOC cells are unveiled, more efforts should be devoted to conducting in vivo assays and revealing their dynamic pharmaceutical influences.

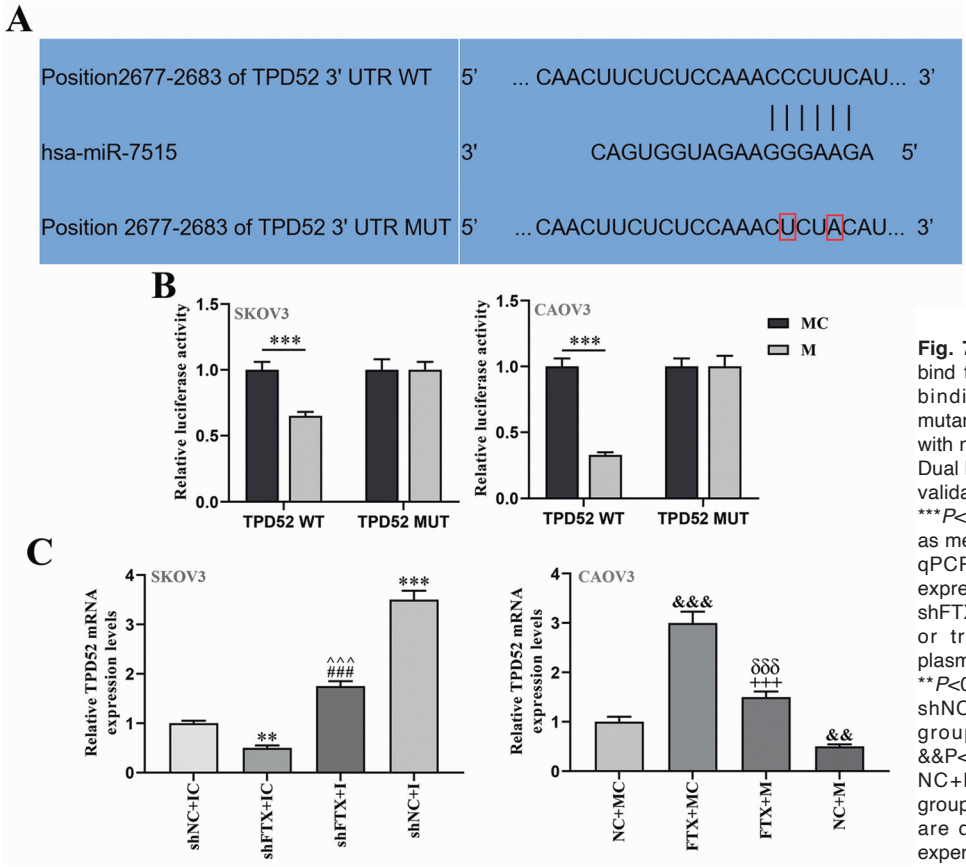

Fig. 7. TPD52 was predicted and validated to bind to miR-7515. **A.** Targetscan predicted the binding of TPD52 with miR-7515. TPD52 mutant sequence (TPD52 MUT) was designed with mutations on the predicted binding sites. **B.** Dual luciferase reporter assay was performed to validate the binding of miR-7515 with TPD52. ***P*<0.001 vs. MC group. Results are described as means ± SD of triplicate experiments. **C.** RT-qPCR assay was conducted to measure the expression of TPD52 in cells transfected with shFTX, miR-7515 inhibitor or their combination, or transfected with FTX overexpression plasmid, miR-7515 mimic or their combination. **P<0.01 vs. shNC+IC group, ***P<0.001 vs. shNC+IC group, ###P<0.001 vs. shFTX+IC group, ^^^P<0.001 vs. shNC+I group, &&P<0.01 vs. NC+MC group, &&&P<0.001 vs. NC+MC group, +++P<0.001 vs. FTX+MC group, δδδP<0.001 vs. NC+M group. Results are described as means ± SD of triplicate experiments.

Acknowledgements. None

Funding. This work was supported by the Nantong Health and Family Planning Commission of Jiangsu (No. WKZL2018088), Nantong University (No.2019LY032) and the Nantong Municipal Health Commission (No. MS2022045 and MA2021022).

Disclosure of Conflict-of-Interest. The authors declare no conflicts of interest.

References

Ali R.H., Kalloger S.E., Santos J.L., Swenerton K.D. and Gilks C.B. (2013). Stage II to IV low-grade serous carcinoma of the ovary is associated with a poor prognosis: A clinicopathologic study of 32 patients from a population-based tumor registry. Int. J. Gynecol. Pathol. 32, 529-535.

Au S.H., Storey B.D., Moore J.C., Tang Q., Chen Y.L., Javaid S., Sarioglu A.F., Sullivan R., Madden M.W., O'Keefe R., Haber D.A., Maheswaran S., Langenau D.M., Stott S.L. and Toner M. (2016). Clusters of circulating tumor cells traverse capillary-sized vessels. Proc. Natl. Acad. Sci. USA 113, 4947-4952.

Byrne J.A., Maleki S., Hardy J.R., Gloss B.S., Murali R., Scurry J.P., Fanayan S., Emmanuel C., Hacker N.F., Sutherland R.L., Defazio A. and O'Brien P.M. (2010). MAL2 and tumor protein D52 (TPD52) are frequently overexpressed in ovarian carcinoma, but differentially associated with histological subtype and patient outcome. BMC Cancer 10, 497.

Calon A., Tauriello D.V. and Batlle E. (2014). TGF-beta in CAF-mediated tumor growth and metastasis. Semin. Cancer Biol. 25, 15-22.

Chang L., Hu Y., Fu Y., Zhou T., You J., Du J., Zheng L., Cao J., Ying M., Dai X., Su D., He Q., Zhu H. and Yang B. (2019). Targeting slug-mediated non-canonical activation of c-Met to overcome chemo-resistance in metastatic ovarian cancer cells. Acta Pharm. Sin. B 9, 484-495.

Chong G.O., Jeon H.S., Han H.S., Son J.W., Lee Y.H., Hong D.G., Lee Y.S. and Cho Y.L. (2015). Differential microRNA expression profiles in primary and recurrent epithelial ovarian cancer. Anticancer Res. 35, 2611-2617.

Dai C., Xie Y., Zhuang X. and Yuan Z. (2018). MiR-206 inhibits epithelial ovarian cancer cells growth and invasion via blocking c-Met/AKT/mTOR signaling pathway. Biomed. Pharmacother. 104, 763-770.

Dean M., Davis D.A. and Burdette J.E. (2017). Activin A stimulates migration of the fallopian tube epithelium, an origin of high-grade serous ovarian cancer, through non-canonical signaling. Cancer Lett. 391, 114-124.

Deng J., Bai X., Feng X., Ni J., Beretov J., Graham P. and Li Y. (2019). Inhibition of PI3K/akt/mTOR signaling pathway alleviates ovarian cancer chemoresistance through reversing epithelial-mesenchymal transition and decreasing cancer stem cell marker expression. BMC Cancer 19, 618.

Doherty J.A., Peres L.C., Wang C., Way G.P., Greene C.S. and Schildkraut J.M. (2017). Challenges and opportunities in studying the epidemiology of ovarian cancer subtypes. Curr. Epidemiol. Rep. 4, 211-220.

Francone E., Gentilli S., Santori G., Stabilini C., Fornaro R. and Frascio M. (2021). MicroRNAs differential expression profile in metastatic colorectal cancer: A pilot study with literature review. Surg. Oncol. 37, 101524.

Guo L., Chen J., Liu D. and Liu L. (2020). OIP5-AS1/miR-137/ZNF217 axis promotes malignant behaviors in epithelial ovarian cancer. Cancer Manag. Res. 12, 6707-6717.

Huang J., Yu Q., Zhou Y., Chu Y., Jiang F. and Wang Q. (2021). FAM201A knockdown inhibits proliferation and invasion of lung adenocarcinoma cells by regulating miR-7515/GLO1 axis. J. Cell Physiol. 236, 5620-5632.

Huang S., Zhu X., Ke Y., Xiao D., Liang C., Chen J. and Chang Y. (2020). LncRNA FTX inhibition restrains osteosarcoma proliferation and migration via modulating miR-320a/TXNRD1. Cancer Biol. Ther. 21, 379-387.

Huo X., Wang H., Huo B., Wang L., Yang K., Wang J., Wang L. and Wang H. (2020). FTX contributes to cell proliferation and migration in lung adenocarcinoma via targeting miR-335-5p/NUCB2 axis. Cancer Cell Int. 20, 89.

Joyce J.A. and Pollard J.W. (2009). Microenvironmental regulation of metastasis. Nat. Rev. Cancer 9, 239-252.

Konecny G.E., Wang C., Hamidi H., Winterhoff B., Kalli K.R., Dering J., Ginther C., Chen H.W., Dowdy S., Cliby W., Gostout B., Podratz K.C., Keeney G., Wang H.J., Hartmann L.C., Slamon D.J. and Goode E.L. (2014). Prognostic and therapeutic relevance of molecular subtypes in high-grade serous ovarian cancer. J. Natl. Cancer Inst. 106, dju249.

Kurman R.J. (2013). Origin and molecular pathogenesis of ovarian high-grade serous carcinoma. Ann. Oncol. 24 (Suppl. 10), x16-21.

Kurman R.J. and Shih Ie M. (2011). Molecular pathogenesis and extraovarian origin of epithelial ovarian cancer-shifting the paradigm. Hum. Pathol. 42, 918-931.

Lee J.M., Yoo J.K., Yoo H., Jung H.Y., Lee D.R., Jeong H.C., Oh S.H., Chung H.M. and Kim J.K. (2013). The novel miR-7515 decreases the proliferation and migration of human lung cancer cells by targeting c-Met. Mol. Cancer Res. 11, 43-53.

Lei S., Zeng Z., He Z. and Cao W. (2021). MiRNA 7515 suppresses pancreatic cancer cell proliferation, migration and invasion via downregulating IGF 1 expression. Oncol. Rep. 46, 200.

Lengyel E. (2010). Ovarian cancer development and metastasis. Am. J. Pathol. 177, 1053-1064.

Lheureux S., Gourley C., Vergote I. and Oza A.M. (2019). Epithelial ovarian cancer. Lancet. 393, 1240-1253.

Li X., Zhao Q., Qi J., Wang W., Zhang D., Li Z. and Qin C. (2018a). LncRNA FTX promotes aerobic glycolysis and tumor progression through the PPARγ pathway in hepatocellular carcinoma. Int. J. Oncol. 53, 551-566.

Li Y., Wu T., Wang Y., Yang L., Hu C., Chen L. and Wu S. (2018b). γ-Glutamyl cyclotransferase contributes to tumor progression in high grade serous ovarian cancer by regulating epithelial-mesenchymal transition via activating PIi3K/AKT/mTOR pathway. Gynecol. Oncol. 149, 163-172.

Li H., Yao G., Zhai J., Hu D. and Fan Y. (2019). LncRNA FTX promotes proliferation and invasion of gastric cancer via miR-144/ZFX axis. Onco Targets Ther. 12, 11701-11713.

Liang H., Yu T., Han Y., Jiang H., Wang C., You T., Zhao X., Shan H., Yang R., Yang L., Shan H. and Gu Y. (2018). LncRNA PTAR promotes EMT and invasion-metastasis in serous ovarian cancer by competitively binding miR-101-3p to regulate ZEB1 expression. Mol. Cancer 17, 119.

Liu H., Deng H., Zhao Y., Li C. and Liang Y. (2018). LncRNA XIST/miR-

34a axis modulates the cell proliferation and tumor growth of thyroid cancer through MET-PI3K-AKT signaling. J. Exp. Clin. Cancer Res. 37, 279.

Liu L., Wu N., Wang Y., Zhang X., Xia B., Tang J., Cai J., Zhao Z., Liao Q. and Wang J. (2019). TRPM7 promotes the epithelial-mesenchymal transition in ovarian cancer through the calcium-related PI3K/AKT oncogenic signaling. J. Exp. Clin. Cancer Res. 38, 106.

Liu S. and Xi X. (2020). LINC01133 contribute to epithelial ovarian cancer metastasis by regulating miR-495-3p/TPD52 axis. Biochem. Biophys. Res. Commun. 533, 1088-1094.

Livak K.J. and Schmittgen T.D. (2001). Analysis of relative gene expression data using real-time quantitative PCR and the 2(-Delta Delta C(T)) Method. Methods 25, 402-408.

Loret N., Denys H., Tummers P. and Berx G. (2019). The role of epithelial-to-mesenchymal plasticity in ovarian cancer progression and therapy resistance. Cancers (Basel) 11, 838.

Lu W., Wan X., Tao L. and Wan J. (2020). Long non-coding RNA HULC promotes cervical cancer cell proliferation, migration and invasion via miR-218/TPD52 axis. Onco Targets Ther. 13, 1109-1118.

McGranahan N. and Swanton C. (2017). Clonal heterogeneity and tumor evolution: Past, present, and the future. Cell. 168, 613-628.

Shi P., Zhang X., Lou C., Xue Y., Guo R. and Chen S. (2020a). Hsa_circ_0084927 regulates cervical cancer advancement via regulation of the miR-634/TPD52 axis. Cancer Manag. Res. 12, 9435-9448.

Shi R., Wu P., Liu M., Chen B. and Cong L. (2020b). Knockdown of lncRNA PCAT6 enhances radiosensitivity in triple-negative breast cancer cells by regulating miR-185-5p/TPD52 axis. Onco. Targets Ther. 13, 3025-3037.

Siegel R.L., Miller K.D. and Jemal A. (2016). Cancer statistics, 2016. CA Cancer J. Clin. 66, 7-30.

Thiery J.P. and Sleeman J.P. (2006). Complex networks orchestrate epithelial-mesenchymal transitions. Nat. Rev. Mol. Cell Biol. 7, 131-142.

Wang G., Ma C., Shi X., Guo W. and Niu J. (2019). MiR-107 enhances the sensitivity of breast cancer cells to paclitaxel. Open Med. (Wars). 14, 456-466.

Wang H., Ni C., Xiao W. and Wang S. (2020a). Role of lncRNA FTX in invasion, metastasis, and epithelial-mesenchymal transition of endometrial stromal cells caused by endometriosis by regulating the PI3K/Akt signaling pathway. Ann. Transl. Med. 8, 1504.

Wang J., Ding W., Xu Y., Tao E., Mo M., Xu W., Cai X., Chen X., Yuan J. and Wu X. (2020b). Long non-coding RNA RHPN1-AS1 promotes tumorigenesis and metastasis of ovarian cancer by acting as a ceRNA against miR-596 and upregulating LETM1. Aging (Albany NY) 12, 4558-4572.

Wang Z., Li Y., Fan L., Zhao Q., Tan B., Liu R. and Li F. (2020c). Silencing of TPD52 inhibits proliferation, migration, invasion but induces apoptosis of pancreatic cancer cells by deactivating Akt pathway. Neoplasma 67, 277-285.

Wu M., Shang X., Sun Y., Wu J. and Liu G. (2020). Integrated analysis of lymphocyte infiltration-associated lncrna for ovarian cancer via TCGA, GTEx and GEO datasets. PeerJ 8, e8961.

Yang W.L., Lu Z. and Bast R.C. Jr (2017). The role of biomarkers in the management of epithelial ovarian cancer. Expert Rev. Mol. Diagn. 17, 577-591.

Ye X. and Weinberg R.A. (2015). Epithelial-mesenchymal plasticity: A central regulator of cancer progression. Trends Cell Biol. 25, 675-686.

Zhang Z., Yao L., Yang J., Wang Z. and Du G. (2018). PI3K/Akt and HIF 1 signaling pathway in hypoxia ischemia (Review). Mol. Med. Rep. 18, 3547-3554.

Zhang R., Shi H., Ren F., Feng W., Cao Y., Li G., Liu Z., Ji P. and Zhang M. (2019). MicroRNA-338-3p suppresses ovarian cancer cells growth and metastasis: Implication of Wnt/catenin beta and MEK/ERK signaling pathways. J. Exp. Clin. Cancer Res. 38, 494.

Zhang F., Wang X.S., Tang B., Li P.A., Wen Y. and Yu P.W. (2020). Long non-coding RNA FTX promotes gastric cancer progression by targeting miR-215. Eur. Rev. Med. Pharmacol. Sci. 24, 3037-3048.

Zhao K., Ye Z., Li Y., Li C., Yang X., Chen Q. and Xing C. (2020). LncRNA FTX contributes to the progression of colorectal cancer through regulating miR-192-5p/EIF5A2 axis. Onco Targets Ther. 13, 2677-2688.

Zhuang J., Lu Q., Shen B., Huang X., Shen L., Zheng X., Huang R., Yan J. and Guo H. (2015). TGFβ1 secreted by cancer-associated fibroblasts induces epithelial-mesenchymal transition of bladder cancer cells through lncRNA-ZEB2NAT. Sci. Rep. 5, 11924.

Accepted January 9, 2023